MOLECULAR AND CELLULAR BIOLOGY, Apr. 2001, p. 2349–2358 Vol. 21, No. 7
0270-7306/01/$04.00+0 DOI: 10.1128/MCB.21.7.2349–2358.2001

Novel Function of Rad27 (FEN-1) in Restricting Short-Sequence Recombination

M. CRISTINA NEGRITTO,[1] JUNZHUAN QIU,[2] DAWN O. RATAY,[1] BINGHUI SHEN,[2] AND ADAM M. BAILIS[1]*

Department of Molecular Biology, Beckman Research Institute,[1] and Department of Cell and Tumor Biology, City of Hope National Medical Center,[2] Duarte, California 91010-0269

Received 1 December 2000/Returned for modification 6 January 2001/Accepted 15 January 2001

Saccharomyces cerevisiae **mutants lacking the structure-specific nuclease Rad27 display an enhancement in recombination that increases as sequence length decreases, suggesting that Rad27 preferentially restricts recombination between short sequences. Since wild-type alleles of both *RAD27* and its human homologue *FEN1* complement the elevated short-sequence recombination (SSR) phenotype of a *rad27*-null mutant, this function may be conserved from yeast to humans. Furthermore, mutant Rad27 and FEN-1 enzymes with partial flap endonuclease activity but without nick-specific exonuclease activity partially complement the SSR phenotype of the *rad27*-null mutant. This suggests that the endonuclease activity of Rad27 (FEN-1) plays a role in limiting recombination between short sequences in eukaryotic cells.**

Dispersed, short (less than 300 bp), repetitive DNA sequences are a dominant feature of all eukaryotic genomes (8). Recombination between these sequences creates a variety of genome rearrangements (45, 61) and can cause disease in humans (12). Discouraging recombination between short sequences enhances genome stability by reducing the incidence of these rearrangements.

In *Saccharomyces cerevisiae* and mammalian cells, short repeats recombine less frequently per unit length than longer sequences (25, 46, 57), while sequences below 30 bp recombine extremely poorly (35). Recent discoveries suggest a genetic basis for the limitation of short-sequence recombination (SSR) in yeast. Novel mutations in the *RAD3, SSL1*, and *SSL2* genes, which encode components of the nucleotide excision repair (NER) apparatus and transcription factor TFIIH (14, 69), disrupt the control of SSR and increase genome rearrangement (2, 3, 29, 34). Genome instability may be due to slow removal of sequences at the ends of broken DNA molecules by an unidentified nuclease or nucleases. The persistence of these sequences increases the likelihood that they will recombine with other sequences in the genome. Interestingly, these factors also influence Ty1 retrotransposition, which gives rise to distinct genome rearrangements (28, 29).

A search for nucleases that affect SSR led us to examine the effects of null alleles of several structurally related nuclease genes in yeast. Previously, it was shown that Rad2, a NER endonuclease (13, 20), does not play a role in SSR (2). Similarly, in this report we describe evidence that Exo1, a 5′-3′ double-stranded exonuclease that plays a role in homologous recombination, mismatch repair, and the repair of UV-damaged DNA (16, 41, 54, 63, 66), and Din7, a mitochondrial protein that affects mitochondrial DNA stability (15), do not significantly affect SSR.

* Corresponding author. Mailing address: Department of Molecular Biology, Beckman Institute of the City of Hope, 1450 E. Duarte Rd., Duarte, CA 91010-0269. Phone: (626) 359-8111, ext. 64031. Fax: (626) 301-8271. E-mail: abailis@coh.org.

Rad27, a fourth, related protein, is a structure-specific endo- and exonuclease homologous to the human FEN-1 enzyme (5, 21, 31, 42, 51, 55, 71). Yeast cells carrying a null allele of the *RAD27* gene display a broad array of defects in genome stability, including an elevated spontaneous mutation rate (64), expansion and contraction of micro- and minisatellite sequences (19, 26, 27, 48, 56), telomeric repeat fluctuation (40), increased spontaneous recombination (19, 32, 55, 64, 67), and increased chromosome breakage (19, 67). These are attributed to a failure in the removal of RNA residues from the 5′ ends of Okazaki fragments during lagging-strand DNA synthesis (19, 64, 67). Importantly, this biochemical defect also affects the repair of DNA double-strand breaks (DSBs) by homologous recombination (22).

Interestingly, a variety of genome rearrangements involving very short (3 to 12 bp) repeats have been observed in *rad27*-null mutant cells but not in wild-type cells (10, 64). These rearrangements could result from aberrant repair of DSBs by homologous recombination. The lethal effect of blocking homologous recombination in *rad27* mutant cells indicates that DSB repair is critical for their survival (59, 64).

In this report we show that Rad27 inhibits the insertion of DNA fragments into the genome, a model for the repair of broken chromosomes (36, 43). Similar to recombination in the *rad3, ssl1*, and *ssl2* mutants described previously (2, 3, 29, 34), SSR was stimulated severalfold in the *rad27*-null mutant, while recombination between long sequences was unaffected.

Complementation of the elevated SSR phenotype by *FEN1* suggests that this function may be conserved from yeast to humans. Interestingly, mutant alleles of *FEN1* and *RAD27* that encode proteins with partial endonuclease activity but no exonuclease activity partially complement the elevated SSR of the *rad27* mutant, indicating that endonuclease activity is required to limit SSR. Further, we show that Rad27 is required to insert DNA fragments with nonhomologous sequences at their ends into genomic sequences by SSR, suggesting that Rad27 plays a role in processing recombining molecules. These results suggest that Rad27 may play a role in maintaining

TABLE 1. Plasmids used in this study

Plasmid	Description	Source or reference
pRS414	Yeast centromere plasmid containing *TRP1* selectable marker	53
pFA6a-kanMX4	Plasmid containing *KAN-MX* selectable marker	68
pET-FEN-1	1.2-kb *FEN1* cDNA in pET28-b for overexpression of FEN-1	18
pET-fen-1-E160D	1.2-kb *fen1-E160D* cDNA in pET28-b for overexpression of FEN-1-E160D	18
pBS-RAD27	1.2-kb *RAD27* PCR clone in pBluescript	This study
pET-RAD27	1.2-kb *RAD27* sequence replaces *FEN1* sequence in pET-FEN-1 for overexpression of Rad27	This study
pET-rad27-E158D	1.2-kb *rad27-E158D* sequence from in vitro-mutagenized pBS-RAD27 in pET28-b for overexpression of Rad27-E158D	This study
pLAY144	1.1-kb *Bam*HI *URA3* sequence replacing 60-bp *BglII* segment of 1.3-kb *HIS3* sequence	2
pLAY266	3.8-kb *Bgl*II/*Bam*HI *hisG*::*URA3*::*hisG* fragment replacing 1.2-kb *Hpa*I/*Eco*RV fragment of *LEU2* sequence in pUC18-LEU2	Glenn Manthey
pLAY281	3.8-kb *Bgl*II/*Bam*HI *hisG*::*URA3*::*hisG* fragment replaces 1.2-kb *Dra*I segment of 2.0-kb *EX01* sequence	This study
pLAY298	3.2-kb *Sac*I fragment carrying the wild-type *FEN1* coding sequence under the control of the yeast *ADH1* promoter and terminator inserted into the polylinker of pRS414	This study
pLAY303	1.5-kb *Apa*I fragment containing the *fen1-E160D* mutation swapped for wild-type *FEN1* sequence in pLAY298	This study
pLAY315	2.0-kb *Hpa*I/*Sma*I *LEU2* sequence replaces 60 bp of *URA3* coding sequence between *Apa*I and *Stu*I sites in pLAY144	This study
pLAY327	1.2-kb PCR-generated *RAD27* coding sequence with *Not*I ends swapped with the 1.2-kb *Not*I fragment carrying the *FEN1* coding sequence in pLAY298	This study
pLAY362	720-bp *Cla*I/*Bst*XI fragment carrying *rad27-E158D* mutation swapped for wild-type sequence in pLAY327	This study
pLAY365	1.5-kb *Bam*HI *TRP1* sequence replacing 60-bp *Bgl*II segment of 1.3-kb *HIS3* sequence	This study

genome stability by cleaving and destabilizing intermediates that are important determinants of the efficiency of SSR.

MATERIALS AND METHODS

Yeast strains and plasmids. Plasmids used in this study were constructed using established methods (47) and are listed in Table 1. Plasmids and DNA fragments were introduced into yeast by electroporation. All yeast strains used in this study were isogenic with W303-1A (62) and are listed in Table 2. The *rad5-535* allele was found to have no effect on the recombination assays performed in this study (unpublished data). Strain construction and maintenance followed established procedures (52). The construction of the *rad27*::*LEU2* allele was described previously (18). The *LEU2* marker in this allele was replaced (44) with the *hisG*::*URA3*::*hisG* universal disruptor (1) by transforming the strain IC2-1 (18) with a 4.9-kb *Xho*I/*Sal*I *leu2*::*hisG*::*URA3*::*hisG* fragment from pLAY266. Ura^+ Leu^- transformants were plated on 5-fluoroorotic acid medium (7) to create the *rad27*::*leu2*::*hisG* allele, which was confirmed on Southern blots (unpublished data). The *exo1*::*hisG*::*URA3*::*hisG* allele was constructed by transforming W961-5A (34) with a 4.6-kb *Xho*I/*Xba*I *exo1*::*hisG*::*URA3*::*hisG* fragment from pLAY281. The *exo1*::*hisG* allele was obtained by 5-fluoroorotic acid selection and confirmed by Southern blot (unpublished data). The *din7*::*KAN-MX* allele was constructed by transforming W1011-3B to G418 resistance (200 μg/ml) with a PCR-generated DNA fragment carrying the *KAN-MX* gene (68) bordered by *DIN7* sequences. The primers 5′-CAATTAAAGAGAATTCAAAAACAGGTG TCCCTGAAAAAATACATGTATCAAACACGTACGCTGCAGGTCGA C-3′ and 5′-CTCCCTCTCCGATAACACGTCCTGCGTATCCACTAGCGGT TGCTCCACTTTCTTATCGATCAATTCGAGCTCG-3′ were used to amplify *KAN-MX* sequences from pFA6a-kanMX4 (68). To construct the *his3*::*ura3*::*LEU2* allele, a 2.0-kb *Hpa*I/*Sma*I *LEU2* clone was inserted into *Stu*I- and *Apa*I-digested pLAY144 (2), bisecting the *URA3* gene in the *his3*::*URA3* segment and creating pLAY315. A 3.2-kb *Hin*dIII fragment from pLAY315 containing the *his3*::*ura3*::*LEU2* segment was used to transform W961-5A to leucine prototrophy. Leu^+ His^- transformants were confirmed to have replaced the wild-type *HIS3* allele with the *his3*::*ura3*::*LEU2* allele by Southern blotting (unpublished data). The *sam2*::*his3*::*TRP1* allele was generated by transforming W961-5A to tryptophan prototrophy with a PCR-generated DNA fragment carrying the *TRP1* gene flanked by 91 and 36 bp of *HIS3* coding sequence bordered on both sides by 45 bp of the *SAM2* coding sequence. The oligonucleotides 5′-GGTCCTCA AGGTGACGCTGGTTTGACCGTAGAAAGATTATTGTCAAGCTTTTAAA ATAGGCCC-3′ and 5′-GGAGAAGGCACCACCACCGACGGATGAGGCA CCACCGTAAGCGTCAAGCTTTCAAGAAAATGC-3′ were used to amplify the *his3*::*TRP1* sequence from pLAY365. Trp^+ transformants were confirmed to have the *sam2*::*his3*::*TRP1* allele by Southern blotting (unpublished data).

Cloning and in vitro mutagenesis of *RAD27* and *FEN1*. The *RAD27* coding sequence was amplified by PCR from yeast genomic DNA using the oligonucleotides 5′-CCCCGGGCCCGCGGCCGCATGGGTATTAAAGGTTTG-3′ and 5′-CCCCGGGCCCGCGGCCGCTCATCTTCTTCCCTTTGT-3′. These primers include *Not*I (underlined) sequences for cloning. The 1.2-kb *RAD27* PCR product was digested with *Not*I and inserted in place of the *FEN1* gene in pLAY298 to create pLAY327 for expression in yeast. This plasmid puts *RAD27* under the control of the *ADH1* promoter and terminator and possesses a centromere and a *TRP1* selectable marker. *RAD27* was also amplified using the oligonucleotides 5′-ACAGCACGCGGCCGC**CATGG**GTATTAAAGGTTTG A-3′ and 5′-ACCTAGGAGCGGCCGCTTA**CTCGAG**TCTTCTTCCCTTTGT GACT-3′, which include *Not*I (underlined) and *Nco*I or *Xho*I (in boldface) sequences. *Nco*I- and *Xho*I-digested *RAD27* PCR product was cloned into *Nco*I- and *Xho*I-digested pET28b and pBluescript to create pET-RAD27 for overexpression in *Escherichia coli* and pBS-RAD27 for in vitro mutagenesis. pBS-RAD27 was mutagenized using the RAPID PCR site-directed mutagenesis kit (Stratagene, La Jolla, Calif.) and the oligonucleotides 5′-CCAACGGAAGCT**G AT**GCTCAATGTGC-3′ and 5′-GCACATTGAGC**ATC**AGCTTCCGTTGG-3′ (substituted codon in bold). The *rad27-E158D* mutation was verified by DNA

TABLE 2. Yeast strains used in this study

Strain	Genotype[a]	Source or reference
W961-5A	*MAT***a** *HIS3*	34
W1011-3B	*MAT*α *HIS3*	John McDonald
IC2-1	*MAT***a** *HIS3 rad27*::*LEU2*	18
ABX367	*MAT***a**/α *HIS3*/*his3*::*ura3*::*LEU2*	This study
ABX382	*MAT***a**/α *HIS3*/*his3*::*ura3*::*LEU2 rad27*::*leu2*::*hisG*/*rad27*::*leu2*::*hisG*	This study
ABX451	*MAT***a**/α *HIS3*/*his3*::*ura3*::*LEU2 din7*::*KAN-MX*/*din7*::*KAN-MX*	This study
ABX456	*MAT***a**/α *HIS3*/*his3*::*ura3*::*LEU2 exo1*::*hisG*/*exo1*::*hisG*	This study
ABX457-2A	*MAT*α *his3*::*ura3*::*LEU2 sam2*::*his3*::*TRP1*	This study
ABX457-1B	*MAT*α *his3*::*ura3*::*LEU2 sam2*::*his3*::*TRP1 rad27*::*leu2*::*hisG*	This study
ABT301	Same as ABX382, with addition of pLAY298 (*FEN1*)	This study
ABT302	Same as ABX382, with addition of pLAY327 (*RAD27*)	This study
ABT303	Same as ABX382, with addition of pLAY303 (*fen1-E160D*)	This study
ABT306	Same as ABX382, with addition of pRS414 (empty plasmid)	This study
ABT344	Same as ABX382, with addition of pLAY362 (*rad27-E158D*)	This study

[a] All strains are isogenic to W303-1A (*MAT***a** *ade2-1 can1-100 his3-11,15 leu2-3,112 trp1-1 ura3-1 rad5-535*) (61). Only deviations from this genotype are listed.

sequencing. A 1.2-kb *Nco*I/*Xho*I *rad27-E158D* fragment was cloned into pET28b to make pET-rad27-E158D and to express Rad27-E158D in *E. coli*. A 710-bp *Cla*I/*Bst*XI *rad27-E158D* fragment was swapped with wild-type sequences in pLAY327 to make pLAY362 and to express Rad27-E158D in yeast. Wild-type FEN-1 was overexpressed in *E. coli* cells from the plasmid pET-FEN-1 (18). pET-fen-1-E160D (18) was used for the overexpression of FEN-1-E160D. Wild-type and mutant *FEN1* genes under the control of the *ADH1* promoter and terminator from pDB20-FEN-1 and pDB20-FEN-1-E160D (18) were inserted into pRS414 to create pLAY298 and pLAY303 and to express the proteins in yeast.

Measurement of flap endonuclease and nick exonuclease activities, enzyme kinetics, and substrate flap-length effects of wild-type and mutant proteins. Protein overexpression and purification from *E. coli* extracts were carried out as described previously (18, 49, 50). Purity of the preparations was assessed on Coomassie blue-stained sodium dodecyl sulfate-polyacrylamide gradient gels. 5′ flap and nicked double-strand substrates were prepared as described in Hosfield et al. (23). Flap endonuclease assays were performed in a volume of 13 μl with 0.5 to 25.0 pmol of ^{32}P-labeled flap substrate, TM buffer (10 mM Tris [pH 8.0], 10 mM $MgCl_2$), and 5 to 40 nmol of wild-type or mutant enzyme. The substrates for the flap-length dependence assay are described in Fig. 3. Substrates were synthesized by the DNA synthesis center of the City of Hope National Medical Center and purified on 15% acrylamide gels as described by Frank et al. (18). Seventy-five nanomoles of FEN-1 was used for all of the flap-length dependence assays. All reactions were incubated at 30°C for 10 min and then quenched with an equal volume of stop solution (U.S. Biochemical Corp., Cleveland, Ohio). The products were resolved on denaturing 15% acrylamide gels and visualized by autoradiography. The percentage of substrate cleaved was determined using the IPLabGel program and was converted to substrate concentration cleaved per unit time as described previously (18). V_{max} and K_m values were determined from double-reciprocal plots of product formed versus substrate concentration (data not shown).

DNA fragment insertion assay. DNA fragments with different lengths of *HIS3* sequence flanking the *URA3* gene were prepared by restriction endonuclease digestion of pLAY144 (2) or by PCR. Phenol-extracted and gel-purified DNA fragments were used to transform diploid cells by electroporation, selecting for expression of *URA3*. Transformation efficiency differed by less than 3.5-fold in wild-type and *rad27* mutant cells.

Recombination between the *his3*::*URA3* fragments and several different genomic sequences (Fig. 1) was distinguished by replica plating to appropriate drop-out media and confirmed by Southern blotting DNA from selected transformants (unpublished data). Recombination at the *HIS3* allele replaces 60 bp of *HIS3* coding sequence with the 1.1-kb *URA3* marker and results in His^- Leu^+ Ura^+ transformants. Recombination at the *his3*::*ura3*::*LEU2* allele replaces a 2-kb *LEU2* marker with 60 bp of *URA3* coding sequence and results in His^+ Leu^- Ura^+ transformants. Recombination at either of the *ura3-1* alleles replaces a point mutation in the *URA3* coding sequence by gene conversion and results in His^+ Leu^+ Ura^+ transformants. The fraction of transformants that were due to gene conversion at the *ura3-1* alleles remained between 50 and 60% in both the wild type and the *rad27* mutant, regardless of the DNA fragment used. However, the ratio of recombination events at the *HIS3* allele versus the *his3*::*ura3*::*LEU2* allele varied significantly with changes in the length of the *HIS3* sequences on the DNA fragments. The mean ratio of insertions at *HIS3* versus *his3*::*ura3*::*LEU2* (H^-/L^-) for each strain was determined from at least five trials. Each trial consisted of a minimum of 400 Ura^+ transformants.

The ratios of DNA fragment insertion into the *HIS3* and *his3*::*ura3*::*LEU2* alleles were not significantly influenced by the lengths of DNA being deleted from or transplaced into the genome during recombination. Very similar ratios were obtained when the smallest *his3*::*URA3* fragment was inserted into the *HIS3* allele, which requires deletion of 60 bp (Fig. 1C), as when it was inserted into the *sam2*::*his3*::*TRP1* allele (see Fig. 3B), which requires deletion of 1.5 kb. We also found that inserting a 1.5-kb *TRP1* marker into the *URA3* sequence of the smallest *his3*::*URA3* fragment did not significantly affect the relative frequencies of recombination with the *HIS3* and *his3*::*ura3*::*LEU2* genomic targets (unpublished data), indicating that transplacing 60 bp of DNA into the *his3*::*ura3*::*LEU2* allele was equivalent to 1.5 kb.

Ectopic recombination between the *ura3-1* alleles at the *URA3* loci and the *his3*::*ura3*::*LEU2* allele at the *HIS3* locus occured at a frequency of $\sim 10^{-7}$ (4), which is 10- to 100-fold lower in frequency than fragment insertion into the *his3*::*ura3*::*LEU2* allele and indicates that it does not interfere with the assay. Frequencies of ectopic recombination between the *leu2-3,112* alleles at the *LEU2* loci and the *his3*::*ura3*::*LEU2* allele should occur at a similarly low frequency and should not interfere with the assay.

Nonhomologous ends assay. *his3*::*URA3* fragments with different lengths of *HIS3* sequence were obtained by PCR using pLAY144 as template. The four primer pairs 5′-AAGCTTTTAAAGAGGCCC-3′ and 5′-AAGCTTTCAAGAAAATGC-3′, 5′-CTCTCGGTCAAGCTTTTA-3′ and 5′-CTAGCCTCTGCAAAGCTT-3′, 5′-GCGGGATTGCTCTCGGTC-3′ and 5′-GGTAATTCTGCTAGCCTC-3′, and 5′-ACTGAAGACTGCGGGATT-3′ and 5′-AACGTGGAGGGTAATTCT-3′ were used to generate *his3*::*URA3* fragments with 91 and 36 bp, 101 and 46 bp, 111 and 56 bp, and 121 and 66 bp of *HIS3* sequence flanking the 1.1-kb *URA3* marker, respectively. PCR products were used to transform haploid wild-type and *rad27* mutant cells by electroporation, selecting for Ura^+ recombinants.

As described above, recombination events at the different genomic targets (see Fig. 3) are distinguishable by replica plating to appropriate drop-out media and were confirmed by Southern blot (unpublished data). Just like the previous assay, recombination with the *his3*::*ura3*::*LEU2* allele at the *HIS3* locus replaces a 2-kb *LEU2* marker with 60 bp of *URA3* coding sequence and results in Trp^+ Leu^- Ura^+ transformants. Recombination with the *sam2*::*his3*::*TRP1* allele at the *SAM2* locus replaces 1.5 kb of *TRP1* coding sequence with the 1.1-kb *URA3* marker and results in Trp^- Leu^+ Ura^+ transformants. The fragments can also recombine with the *ura3-1* allele at the *URA3* locus. Fragment recombination at the *URA3* locus remained between 25 and 30% of the total, regardless of fragment length or cell type. However, the ratio of insertions at the *sam2*::*his3*::*TRP1* and *his3*::*ura3*::*LEU2* targets changed significantly depending on the length of the *HIS3* sequences on the fragment. The mean ratio of insertions into the *sam2*::*his3*::*TRP1* and *his3*::*ura3*::*LEU2* targets (T^-/L^-) was determined from at least five trials. Each trial involved a minimum of 400 Ura^+ transformants.

RESULTS

DNA fragment insertion assay. We used the insertion of DNA fragments into the genome to study the effect of DNA sequence length on homologous recombination in wild-type and mutant yeast. This approach was chosen because DNA fragment length can be readily changed and because DNA fragment insertion is similar to the repair of broken chromosomes by homologous recombination (30, 36, 38). In this assay, homozygous wild-type and *rad27* mutant diploids were transformed with three different DNA fragments consisting of a *URA3* marker flanked by varying lengths of *HIS3* sequence. The two relevant genomic targets for the *his3*::*URA3* fragments were a wild-type *HIS3* allele on one copy of chromosome XV and the *his3*::*ura3*::*LEU2* allele on the other (Fig. 1A). Insertion of a fragment into the *HIS3* allele is governed only by the short *HIS3* sequences at its ends, while insertion into the *his3*::*ura3*::*LEU2* allele utilizes its entire length. The length of the terminal *HIS3* sequences on the three fragments, and therefore homology to the *HIS3* allele, varies over 3.5-fold (Fig. 1B). However, overall fragment length and homology to the *his3*::*ura3*::*LEU2* allele vary less than 21% (Fig. 1B). Since significant changes in terminal *HIS3* sequence length have little effect on overall fragment length, the three fragments should have a significantly different propensity to recombine with the *HIS3* allele but a similar propensity to recombine with the *his3*::*ura3*::*LEU2* allele. Therefore, the ratio of DNA fragment insertions into the *HIS3* allele versus the *his3*::*ura3*::*LEU2* allele (H^-/L^-) indicates how well the cell can use the terminal *HIS3* sequences for recombination.

SSR is increased in *rad27* but not *exo1* or *din7* mutant cells. It was previously shown that Rad2 does not play a role in the control of SSR (2). Here we show that SSR was unaffected by the loss of the structurally similar proteins Din7 and Exo1, as the H^-/L^- ratios obtained with fragment 1 (Fig. 1B), which has the shortest *HIS3* ends (127 bp total), were not significantly different from that of the wild type in *exo1*- and *din7*-null mutant cells (Table 3). In contrast, we found that the H^-/L^-

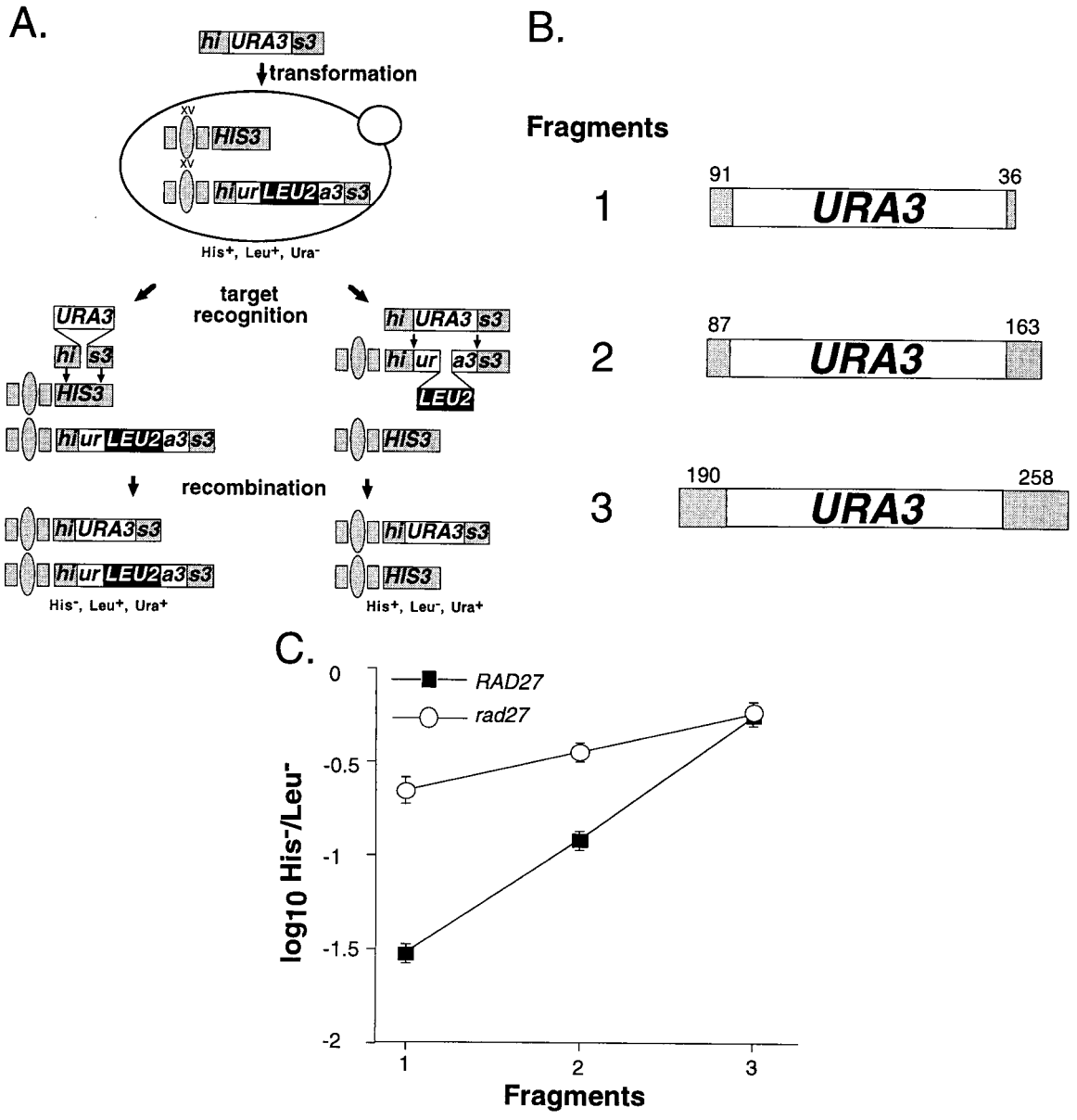

FIG. 1. DNA fragment insertion into the genomes of wild-type and *rad27*-null mutant cells. (A) DNA fragment insertion assay. DNA fragments containing a 1.1-kb *URA3* clone flanked by various lengths of *HIS3* sequence (*his3*::*URA3*) were electroporated into diploid yeast cells. The two relevant recombination targets are a wild-type *HIS3* allele at the *HIS3* locus on one copy of chromosome XV and a *his3*::*ura3*::*LEU2* allele at the *HIS3* locus on the homologue. Alignment of the *his3*::*URA3* fragment with the wild-type *HIS3* allele involves only the terminal *HIS3* sequences, whereas alignment with the *his3*::*ura3*::*LEU2* allele involves all of the fragment. Insertion of the fragment into the *HIS3* allele by recombination replaces 60 bp of the *HIS3* coding sequence with the 1.1-kb *URA3* marker, resulting in a cell that is His^- Leu^+ Ura^+, whereas insertion into the *his3*::*ura3*::*LEU2* allele replaces a 2.0-kb *LEU2* marker with 60 bp of *URA3* sequence that results in a His^+ Leu^- Ura^+ cell. (B) DNA fragments used in the insertion assay. The three *his3*::*URA3* DNA fragments used in the experiments are depicted. The *HIS3* sequences at the ends of the fragments are depicted as shaded boxes with sequence lengths marked above in base pairs. The *URA3* sequence in each fragment is 1,071 bp long. (C) A plot of the ratio of DNA fragment insertions of each *his3*::*URA3* fragment into the *HIS3* and *his3*::*ura3*::*LEU2* targets in wild-type and *rad27* mutant diploids. The three different *his3*::*URA3* fragments were separately electroporated into wild-type (ABX367) and *rad27* homozygous (ABX382) diploids. Ura^+ transformants were replica plated to medium lacking His or Leu to determine which transformants were due to insertion into the *HIS3* or *his3*::*ura3*::*LEU2* alleles. The mean ratios of His^- Leu^+ Ura^+ to His^+ Leu^- Ura^+ transformants (H^-/L^-) obtained with the three DNA fragments were determined from a minimum of 10 independent trials with each fragment in each strain. Log_{10} values of the mean ratios ± two standard errors were plotted for each of the fragments.

ratio in *rad27*-null mutant cells was sevenfold higher than that of the wild type, indicating that Rad27 suppresses recombination between short sequences (Table 3). However, the stimulation was only threefold with fragment 2, which has 250 bp of *HIS3* sequence, and nonexistent with fragment 3, which has 448 bp of *HIS3* sequence (Fig. 1C). Therefore, in this assay *rad27* stimulates recombination between short sequences but not long ones.

The flap endonuclease activities of Rad27 and FEN-1 are implicated in the control of SSR. Previous studies have shown

TABLE 3. SSR phenotypes of wild-type and nuclease-deficient cells

Genotype	H^-/L^- ratio[a]
Wild-type diploid	0.03 ± 0.01
din7::*KANMX*/*din7*::*KANMX*	0.03 ± 0.01
exo1::*hisG*/*exo1*::*hisG*	0.048 ± 0.01
rad27::*leu2*::*hisG*/*rad27*::*leu2*::*hisG*	0.22 ± 0.04

[a] Diploid strains ABX367, ABX382, ABX451, and ABX456 were transformed with the shortest DNA fragment, which contains 91 and 36 bp of DNA flanking the *URA3* gene. The ratio of transformants that were due to fragment insertion into the *HIS3* allele (His^- Leu^+ Ura^+) versus those that were due to insertion into the *his3*::*ura3*::*LEU2* allele (His^+ Leu^- Ura^+) was determined as described in the text. The means from a minimum of five trials ± two standard errors are reported. Means that differ by greater than two standard errors are different at the 95% confidence level.

that mutating a conserved glutamate at residue 160 in the active site of human FEN-1 leads to marked changes in DNA binding and/or 5′ flap cleavage (18, 50). Substituting an aspartate for the glutamate (E160D) has no effect on substrate binding but partially reduces 5′ flap cleavage efficiency (18). Here we show that FEN-1-E160D and the analogous Rad27 mutant enzyme (E158D) possess similar partial flap endonuclease activities (Table 4). The K_ms of FEN-1-E160D and Rad27-E158D for the 5′ flap substrate were nearly equivalent to that of the wild type, but the V_{max}s of FEN-1-E160D and Rad27-E158D were only 59 and 69%, respectively, of that of the wild type. Neither mutant protein possessed any measurable capacity for exonucleolytic cleavage (Table 4). These results demonstrate that the enzymatic functions defined by these assays are separable.

Recently, the human *FEN1* gene was shown to fully complement the temperature-sensitive growth and methyl methanesulfonate sensitivity of the *rad27*-null mutant, while the *fen1-E160D* allele only partially complemented it (18). These results suggest that the cellular functions of these proteins may be conserved and are linked to flap endonuclease activity. We tested whether *FEN1* also complements the SSR phenotype of the *rad27* mutant by comparing the H^-/L^- ratio from *rad27* cells containing *FEN1* on a plasmid to the wild-type ratio. We found that the ratios were not significantly different, demonstrating that *FEN1* complements the SSR phenotype of *rad27*-null mutant cells (Table 5). Interestingly, the ratios obtained with the *fen1-E160D* and *rad27-E158D* mutant alleles were significantly above those from cells containing wild-type *FEN1*

TABLE 4. 5′-Flap endonuclease and 5′-nick-specific exonuclease activities of wild-type and mutant FEN-1 and Rad27 enzymes

Enzyme[a]	Flap endonuclease[b]		Nick exonuclease[c]	
	K_m (nM)	V_{max} (nM/min)	K_m (nM)	V_{max} (nM/min)
Rad27	48.0	3.37	47.5	2.9
Rad27-E158D	48.9	2.33	>150	<0.1
FEN-1	48.1	3.07	47.2	2.3
FEN1-E160D	48.6	1.82	>150	<0.1

[a] Wild-type and mutant enzymes were prepared as described previously (18, 48, 49) and in the text.

[b] From 5 to 40 nmol of enzyme was reacted with 0.1 to 25 pmol of ^{32}P-labeled flap substrate prepared as described previously (23). Double-reciprocal plots of reaction velocities, determined as described previously (18), versus substrate concentrations were used to determine the values for K_m and V_{max}.

[c] From 5 to 40 nmol of enzyme was reacted with 0.1 to 25 pmol of ^{32}P-labeled nicked duplex DNA substrate prepared as described previously (23). The values for K_m and V_{max} were determined as described above.

TABLE 5. Complementation of the *rad27* SSR phenotype by alleles of *FEN1* and *RAD27*

Allele on plasmid[a]	H^-/L^- ratio[b]
None	0.18 ± 0.04
RAD27	0.05 ± 0.006
rad27-E158D	0.08 ± 0.004
FEN1	0.04 ± 0.003
fen1-E160D	0.10 ± 0.01

[a] All strains are *rad27*::*leu2*::*hisG*/*rad27*::*leu2*::*hisG* homozygotes. All plasmids are derived from pRS414, which carries a yeast centromere and a *TRP1* selectable marker (52). Expression of the *FEN1* and *RAD27* alleles is under the control of the yeast *ADH1* promoter and terminator.

[b] Strains ABT301, ABT302, ABT303, ABT306, and ABT344 were transformed with a *his3*::*URA3* fragment that contains 91 and 36 bp of *HIS3* DNA flanking the *URA3* gene. H^-/L^- ratios were determined as described in the text. The means from a minimum of 10 trials ± two standard errors are reported. Means that differ by greater than two standard errors are different at the 95% confidence level.

and *RAD27* but significantly below the ratio obtained from cells containing an empty plasmid (Table 5). Since the intermediate level of complementation by the *fen1-E160D* and *rad27-E158D* alleles matches the flap endonuclease activity data described above (Table 4) and since the levels of Rad27 or FEN-1 protein are similar in cells containing either the wild-type or mutant alleles (data not shown), we suggest that the effects of Rad27 and FEN-1 on SSR are a function of their flap endonuclease activities but not their nick exonuclease activities. In support of these results we found that exonucleolytic degradation at DSBs in *rad27* cells was not significantly different from that in wild-type cells (data not shown).

Length dependence of 5′ flap cleavage. Bambara and colleagues showed that 5′ flap cleavage by FEN-1 requires that the flap remain single stranded until its junction with duplex DNA (37). This implies that the enzyme must slide unimpeded from the 5′ end of the flap to the junction with duplex DNA. We examined the capacity of FEN-1 to cleave flaps of various lengths (Fig. 2). The flaps were comprised of different lengths of oligodeoxythymidine in order to minimize secondary structure formation (11). We found that flap cleavage efficiency decreased markedly with increasing flap length, from 80% cleavage with a 20-bp flap to 28% with a 120-bp flap. Given the very similar in vitro activities of FEN-1 and Rad27 (see Fig. 4), we expect that Rad27 would display similar characteristics. As discussed below, the diminished capacity of FEN-1 and Rad27 to cleave long flaps might in part explain why losing Rad27 preferentially affects SSR.

Rad27 is required for removal of nonhomologous ends during SSR. Previously, Fishman-Lobell and Haber (17) found that a null mutation in the *RAD1* gene blocks recombination when sequences at the ends of DSBs obscure homology with a recombination partner. Subsequently, it was shown that Rad1-Rad10 is a structure-specific endonuclease (58, 65) that can cleave terminal 3′ single strands displaced when adjacent sequences pair with homologous sequences on another DNA molecule (6). Rad1 may cleave other intermediates during several different types of recombination events (2, 60).

Since Rad27 cleaves 5′ single strands at the junction with double-stranded DNA (31), a second DNA fragment insertion assay was designed to test whether it also plays a role in removing nonhomologous sequences from the ends of DNA molecules undergoing homologous recombination (Fig. 3A),

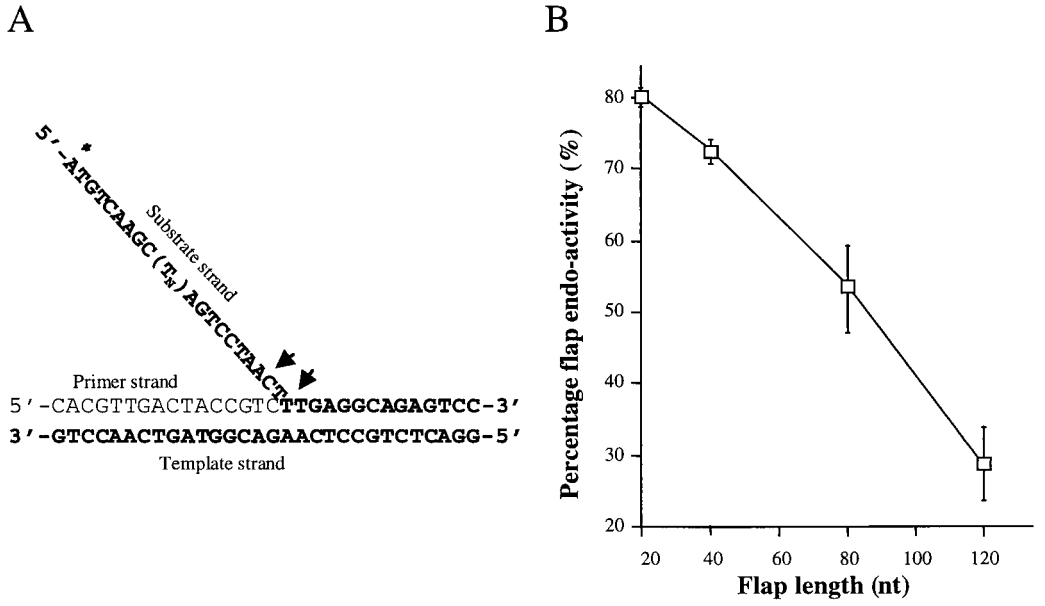

FIG. 2. Effect of DNA flap length on FEN-1 activity. (A) DNA substrates. The substrate consists of three DNA strands. (T_n) indicates the number of T residues (0, 20, 60, or 100) in the substrate strand. This corresponds to total flap lengths of 20, 40, 80, and 120 nucleotides. The asterisk denotes the location of the ^{32}P label. (B) Plot of flap endonuclease activities with different flap lengths. Five picomoles of ^{32}P-labeled flap substrate was incubated with 75 nmol of FEN-1, and reaction products were run on analytical gels and autoradiographed. Substrate and product levels were quantitated by densitometry and converted to cleavage efficiencies by dividing product signals by the total of the substrate and product signals and multiplying by 100. nt, nucleotides.

perhaps implying a role in the processing of other recombination intermediates. Four different DNA fragments consisting of a *URA3* marker bordered by varying lengths of *HIS3* sequence were used to transform haploid wild-type and *rad27*-null mutant cells. One recombination target is the *his3*::*ura3*::*LEU2* allele described above (Fig. 1A). All of the fragments are homologous to this target along their entire length. The other relevant target, *sam2*::*his3*::*TRP1*, consists of a *TRP1* marker bordered by 36- and 91-bp *HIS3* segments at the *SAM2* locus on chromosome IV. The smallest *his3*::*URA3* fragment has the same *HIS3* sequences as the *sam2*::*his3*::*TRP1* target, while the other fragments have 10, 20, or 30 bp of additional *HIS3* sequences at both ends. Recombination between the smallest fragment and *sam2*::*his3*::*TRP1* is unblocked, whereas insertion of the other fragments into this target requires that 10, 20, or 30 bp of terminal *HIS3* sequences be removed from both ends. The different *his3*::*URA3* fragments have the same length of homology with the *sam2*::*his3*::*TRP1* target, and their homology with the *his3*::*ura3*::*LEU2* target varies very little (less than 5%). Since there is little difference in the lengths of homology shared by the fragments and the targets, this should have little effect on the ratios of fragment insertion into the two targets (T^-/L^-). Therefore, changes in these ratios should indicate how well the cell can remove any excess *HIS3* sequences from the ends of a fragment during recombination with the *sam2*::*his3*::*TRP1* target (Fig. 4B).

The results of these assays indicate that Rad27 plays an important role in the removal of nonhomologous sequences from the ends of recombining DNA molecules. Each addition of 10 bp of nonhomologous sequences onto the ends of the DNA fragments decreased insertion into the *sam2*::*his3*::*TRP1* target relative to the *his3*::*ura3*::*LEU2* target approximately twofold in *rad27* mutant cells (Fig. 3B). The nonhomologous sequences had much less of an impact on the ratio of insertion into the two targets in wild-type cells, as the addition of 10 bp of nonhomologous sequences had no effect and even of 30 bp had little more than a twofold effect (Fig. 3B). Therefore, the presence of Rad27 facilitates the removal of sequences that can otherwise inhibit recombination. Since the exonuclease activity of Rad27 appears to play little, if any, role in the control of SSR (Table 4; data not shown), we conclude that the 5′ flap endonuclease of Rad27 can cleave flaps that form at the ends of recombining molecules.

DISCUSSION

Previous work with several mutants demonstrated a correlation between increased DSB stability and enhanced frequencies of SSR (2, 3, 29, 34). This led to the investigation of how null alleles of several nuclease genes affect SSR. A novel DNA fragment insertion assay was used to show that the *exo1* and *din7* alleles have negligible effects on SSR (Table 3), while the *rad27* allele confers a significant increase in SSR (Fig. 1). Combined with results previously obtained with a *rad2* mutant (34), these data support the conclusion that *RAD27* is the only member of this group of genes that plays a significant role in the control of SSR.

Our assay for *his3*::*URA3* fragment insertion into genomic *HIS3* sequences does not require that the recombination events perfectly conserve the homology between the fragment and genomic sequences. Since *rad27* mutants accumulate mutations that appear to be due to imprecise recombination (64), we examined the precision of fragment insertion events in *rad27* mutant cells. Analysis of the DNA sequences of 40

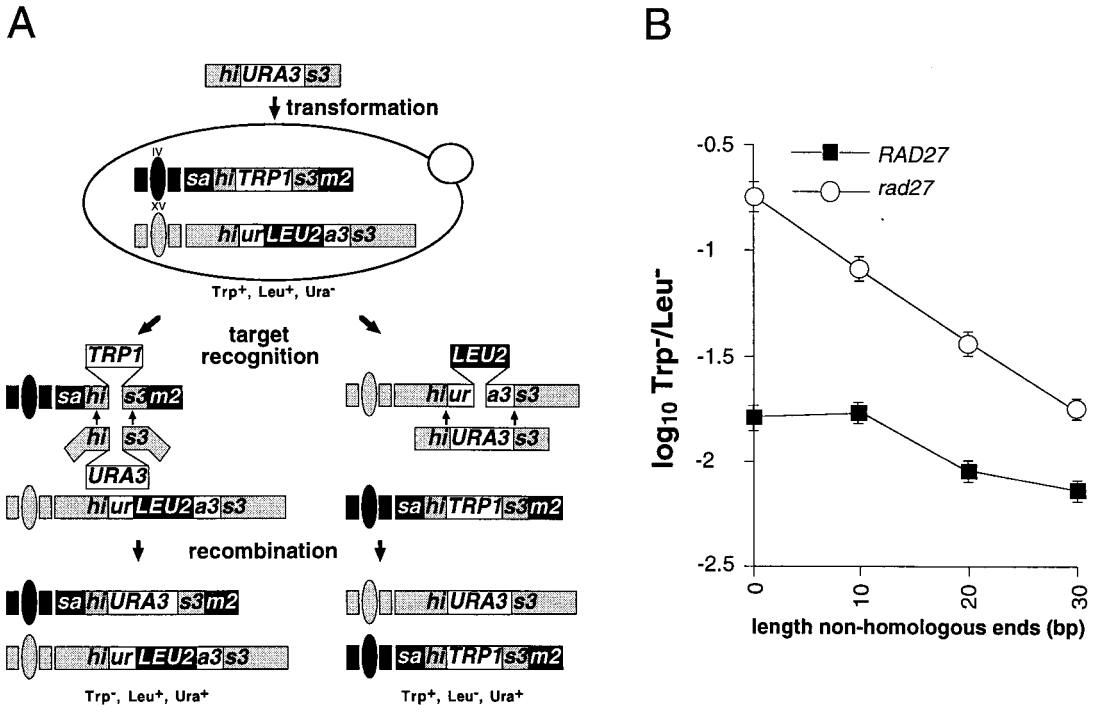

FIG. 3. Relationship between length of nonhomologous DNA sequences at ends of substrate DNA fragments and their integration into genomes of wild-type and *rad27*-null mutant cells. (A) DNA fragment insertion assay involving nonhomologous terminal sequences. DNA fragments comprised of the *URA3* gene bordered by various lengths of *HIS3* sequence were introduced into haploid cells by electroporation. The two relevant recombination targets are the previously described *his3*::*ura3*::*LEU2* allele at the *HIS3* locus on chromosome XV and the *sam2*::*his3*::*TRP1* allele at the *SAM2* locus on chromosome IV. All of the sequences on the fragments can align with the *his3*::*ura3*::*LEU2* allele, whereas only the *HIS3* sequences can align with the *sam2*::*his3*::*TRP1* allele. All of the *HIS3* sequences on the smallest *his3*::*URA3* fragment (127 bp) can align with the *HIS3* sequences in the *sam2*::*his3*::*TRP1* allele (not pictured), while the +10, +20, and +30 fragments have an additional 10, 20, or 30 bp of *HIS3* sequence at both ends that cannot. These nonhomologous ends must be removed for insertion into the *sam2*::*his3*::*TRP1* allele to occur. Insertion into the *his3*::*ura3*::*LEU2* allele deletes the 2.0-kb *LEU2* sequence, which results in a Trp^+ Leu^- Ura^+ cell, while insertion into the *sam2*::*his3*::*TRP1* allele deletes the 1.5-kb *TRP1* sequence and creates a Trp^- Leu^+ Ura^+ cell. (B) Plot of the ratio of DNA fragment insertions into the *sam2*::*his3*::*TRP1* and *his3*::*ura3*::*LEU2* targets versus length of terminal *HIS3* sequence on the fragment that is not homologous to *sam2*::*his3*::*TRP1* in wild-type and *rad27* mutant cells. The four different *his3*::*URA3* fragments were separately introduced into wild-type (ABX457-2A) and *rad27* mutant (ABX457-1B) cells by electroporation. Ura^+ transformants were replica plated to media lacking tryptophan or leucine to determine whether the fragments had inserted into the *sam2*::*his3*::*TRP1* allele or the *his3*::*ura3*::*LEU2* allele. The mean ratios of Trp^- Leu^+ Ura^+ to Trp^+ Leu^- Ura^+ transformants (T^-/L^-) obtained with the four DNA fragments were determined from a minimum of five independent trials. Log_{10} values of the mean ratios ± two standard errors were plotted against the length of the nonhomologous sequences at the ends of the fragment.

independent insertions of the smallest *his3*::*URA3* fragment into the *HIS3* allele of *rad27* cells revealed no alterations of the *HIS3* sequences undergoing recombination (data not shown). In combination with the observation that no fragment insertion is obtained in cells lacking Rad52 (G. Manthey and A. Bailis, unpublished observations), a central factor in homologous recombination (39), we suggest that the loss of Rad27 stimulates precise recombination between short sequences by a Rad52-dependent mechanism.

The biological functions of FEN-1 and Rad27 may be conserved, since the expression of human *FEN1* in *rad27* mutant yeast cells complements their temperature-sensitive growth, methyl methanesulfonate sensitivity, and elevated SSR (18) (Table 5). This apparent conservation is both structural and functional, as changing conserved glutamate residues to aspartates in both proteins leads to similar changes in enzymatic activity (Table 4). Since the mutant alleles partially complement the *rad27* SSR phenotype (Table 5), we conclude that the endonuclease activities of Rad27 and FEN-1 are important for SSR control in yeast and, perhaps, human cells. While the effect of mutations in genes that encode TFIIH-NER core proteins on SSR correlates with defects in DSB processing (2, 3, 29, 34), the loss of Rad27 has no impact on the exonucleolytic degradation of DSBs (data not shown). This suggests that Rad27 may restrict SSR by a mechanism that is different from that of the TFIIH-NER apparatus. We are currently testing this by epistasis analysis.

We found that Rad27 is needed for efficient SSR when the DNA fragment has sequences at both ends that are not homologous to the genomic target (Fig. 3), implying that Rad27 cleaves 5′ overhangs that block SSR. This is similar to the observation by Wu et al. (70) that 5′ overhang removal by Rad27 appears to be important in the recovery of certain nonhomologous end-joining (NHEJ) products. Both results imply that basepairing, or heteroduplex formation, precedes trimming of 5′ tails from recombining molecules. Therefore, unlike recombination between long, homologous sequences, SSR does not seem to require prior degradation of the 5′ ends of DNA molecules (39). Interestingly, nonhomologous sequences at the ends of DNA fragments that shared hundreds

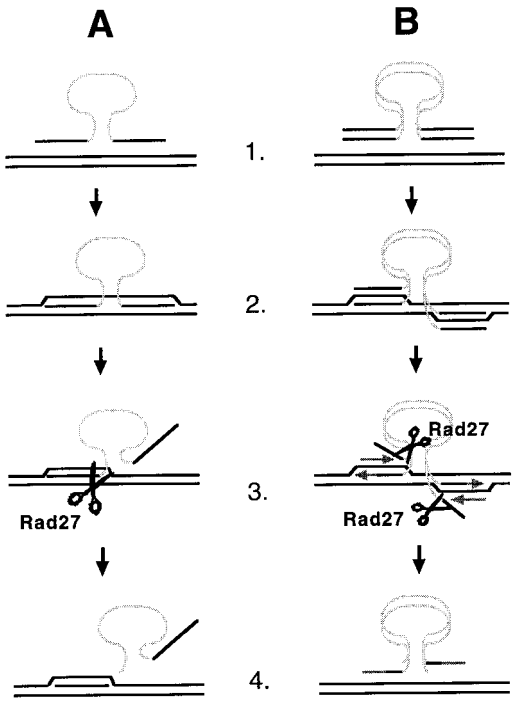

FIG. 4. Models of how Rad27 and FEN-1 may limit recombination between short sequences. (A) Single-strand assimilation. 1. A single strand of the *his3*::*URA3* fragment is pictured with *HIS3* genomic target sequences. *HIS3* sequences are represented by black lines and *URA3* sequences are represented by a gray line. 2. A single strand of the *his3*::*URA3* fragment invades homologous genomic sequences, creating a heteroduplex. 3. Short heteroduplexes may be unwound by a helicase(s). The unannealed 5′ single strand is a substrate for endonucleolytic cleavage by Rad27. 4. Recombination is aborted. (B) Break-induced repair. 1. A double-stranded *his3*::*URA3* fragment is pictured with *HIS3* genomic target sequences. *HIS3* sequences are represented by black lines and *URA3* sequences are represented by light gray lines. 2. The ends of the double-stranded *his3*::*URA3* fragment invade *HIS3* genomic sequences, forming four-stranded heteroduplex intermediates. 3. The short heteroduplexes may be unwound by the advancing lagging-strand polymerase or by a helicase(s), creating unannealed 5′ single strands that are cleaved by Rad27. 4. Recombination is aborted because the unannealed 5′ strands of the DNA fragment have been cleaved away, leaving the newly synthesized Okazaki fragments unable to ligate onto the ends of the fragment.

of base pairs of homology with their genomic targets had no effect on fragment insertion in wild-type or *rad27* mutant cells (M. Navarro and A. Bailis, unpublished observations). This implies that nonhomologous 5′ tails can be removed by a Rad27-independent mechanism during recombination between longer sequences. We speculate that this process may remove RNA primer residues from the 5′ ends of newly synthesized DNA molecules in the absence of Rad27.

Why is recombination between short sequences, but not long sequences, increased in the *rad27* mutant? Genomic DSB formation is enhanced in *rad27* mutants, which increases the incidence of many recombination events (10, 19, 64). In our assays, an increase in the frequency of DSBs at the genomic targets is just as likely to increase recombination with the longer DNA fragments as with the shorter DNA fragments. However, the genome-wide increase in DSBs in *rad27* mutant cells may deplete the factors that normally suppress the insertion of DNA fragments into the genome by SSR. Alternatively, the failure by *rad27* cells to remove nonhomologous sequences from the ends of recombining DNA molecules (Fig. 4) suggests that Rad27 might restrict recombination at a stage following the formation of DSBs. For example, following heteroduplex formation, Rad27 might remove unannealed 5′ single strands generated by an advancing lagging-strand polymerase or helicase unwinding (33). The TFIIH-NER helicases Rad3 and Ssl2, which play a role in SSR control (2, 3, 29, 34), and Dna2, a helicase that works in concert with Rad27 during DNA replication (9), are potential candidates for this activity. If unwinding is extensive, Rad27 could remove enough DNA to terminate recombination as discussed below. Decreasing the length of the sequences shared by the recombination partners would increase the likelihood of complete heteroduplex unwinding, 5′ flap cleavage (Fig. 2), or both.

Several existing models for DNA fragment insertion into the genome (30, 36, 39, 43) were used to construct models for how Rad27 may restrict SSR. The first model (Fig. 4A) is based on the single-strand assimilation model of Leung et al. (30). Following formation of a heteroduplex between a single strand of the DNA fragment and genomic sequences, helicase unwinding creates a 5′ flap that includes the selectable marker. Flap cleavage by Rad27 would terminate recombination because the fragment containing the marker would not have homology to the genomic target on both sides. An important caveat limiting the attractiveness of this model is that the 5′ flap would exceed 1 kb and be a poor substrate for Rad27 (Fig. 2). We favor another model (Fig. 4B) based on the break-copy model of Morrow et al. (36), which is similar to the break-induced repair model for the repair of genomic DSBs (39). Following heteroduplex formation between the ends of the DNA fragment and the genomic target, the ends of the fragment simulate the ends of broken chromosomes by copying genomic sequences. DNA fragment insertion is concluded when the replication forks reach the centromere or the end of the chromosome or by Holliday junction resolution at nicks or gaps. Recombination could be impeded by unwinding the heteroduplex and cleaving the resulting 5′ flap before an Okazaki fragment can be ligated onto the 5′ strand. This would terminate fragment insertion unless the lagging-strand polymerase switches from a chromosomal template to the DNA fragment, which would be unlikely to occur if the remaining heteroduplex between the 3′ strand and the target is also unstable.

Kolodner and colleagues observed genome rearrangements involving very short repeats in *rad27* mutant cells that were not observed in wild-type cells (10, 64). We have observed that deletions between 100-bp repeats are fourfold more stimulated in *rad27* mutant cells than deletions between 400-bp repeats (unpublished data). These results suggest that Rad27 plays a role in limiting recombination between an abundant class of genomic sequences which could contribute to the etiology of cancer. Previously, it was suggested that Rad27 limits recombination by limiting DSB formation (19, 59, 64). In addition, the work described here suggests that Rad27 and FEN-1 restrict SSR by processing recombination intermediates. Armed with the evolving understanding of the relationship between FEN-1 and its substrates at the atomic level (23, 24), our future studies will continue to focus on the molecular details of how Rad27 and FEN-1 maintain genome stability.

ACKNOWLEDGMENTS

This work was supported by U.S. Public Health Service grants GM57484 to A.M.B. and CA73764 to B.S. and by an APRC suppplemental grant (CA85344) to B.S. and A.M.B. from the National Institutes of Health, as well as by funds from the Beckman Research Institute of the City of Hope and the City of Hope National Medical Center.

We thank J. McDonald for yeast strain W1011-3B and D. Garfinkel, J. Wilson, and several anonymous reviewers for comments on the manuscript. We also thank J. Termini, T. Krontiris, R. J. Lin, J. Haber, D. Gordenin, S. Rosenberg, G. Smith, R. Rothstein, D. Botstein, and the members of the Bailis and Shen laboratories for stimulating discussions.

REFERENCES

1. **Alani, E., L. Cao, and N. Kleckner.** 1987. A method for gene disruption that allows repeated use of *URA3* selection in the construction of multiply disrupted yeast strains. Genetics **116:**541–545.
2. **Bailis, A. M., and S. Maines.** 1996. Nucleotide excision repair gene function in short-sequence recombination. J. Bacteriol. **173:**2136–2140.
3. **Bailis, A. M., S. Maines, and M. C. Negritto.** 1995. The essential helicase gene *RAD3* suppresses short-sequence recombination in *Saccharomyces cerevisiae*. Mol. Cell. Biol. **15:**3998–4008.
4. **Bailis, A. M., and R. Rothstein.** 1990. A defect in mismatch repair in *Saccharomyces cerevisiae* stimulates ectopic recombination between homologous genes by an excision repair dependent process. Genetics **126:**535–547.
5. **Bambara, R. A., R. S. Murante, and R. A. Henricksen.** 1997. Enzymes and reactions at the eukaryotic DNA replication fork. J. Biol. Chem. **272:**4647–4650.
6. **Bardwell, A. J., L. Bardwell, A. E. Tomkinson, and E. C. Friedberg.** 1994. Specific cleavage of model recombination and repair intermediates by the yeast Rad1-Rad10 DNA endonuclease. Science **265:**2062–2065.
7. **Boeke, J. D., F. LaCroute, and G. R. Fink.** 1984. A positive selection for mutants lacking orotidine-5′-phosphate decarboxylase activity in yeast: 5-fluoro-orotic acid resistance. Mol. Gen. Genet. **197:**345–346.
8. **Britten, R. J., and D. E. Kohne.** 1968. Repeated sequences in DNA. Hundreds of thousands of copies of DNA sequences have been incorporated into the genomes of higher organisms. Science **161:**529–540.
9. **Budd, M. E., and J. L. Campbell.** 1997. A yeast replicative helicase, Dna2 helicase, interacts with yeast FEN-1 nuclease in carrying out its essential function. Mol. Cell. Biol. **17:**2136–2142.
10. **Chen, C., and R. D. Kolodner.** 1999. Gross chromosomal rearrangements in *Saccharomyces cerevisiae* replication and recombination deficient mutants. Nat. Genet. **23:**81–85.
11. **Cheng, D. M., M. M. Dhingra, and R. H. Sarma.** 1978. Spatial configuration of deoxyribotrinucleoside diphosphate in aqueous solution. Nucleic Acids Res. **5:**4399–4416.
12. **Deininger, P. L., and M. A. Batzer.** 1999. Alu repeats and human disease. Mol. Genet. Metab. **68:**183–193.
13. **de Laat, W. L., N. G. J. Jaspers, and J. H. J. Hoeijmakers.** 1999. Molecular mechanism of nucleotide excision repair. Genes Dev. **13:**768–785.
14. **Feaver, W. J., J. Q. Svejstrup, L. Bardwell, A. J. Bardwell, S. Buratowski, K. D. Gulyas, T. F. Donahue, E. C. Friedberg, and R. D. Kornberg.** 1993. Dual roles of a multiprotein complex from *Saccharomyces cerevisiae* in transcription and DNA repair. Cell **75:**1379–1387.
15. **Fikus, M. U., P. A. Mieczkowski, P. Koprowski, J. Rytka, E. Sledziewska-Gojska, and Z. Ciesla.** 2000. The product of the DNA damage-inducible gene of *Saccharomyces cerevisiae, DIN7*, specifically functions in mitochondria. Genetics **154:**73–81.
16. **Fiorentini, P., K. N. Huang, D. X. Tishkoff, R. D. Kolodner, and L. S. Symington.** 1997. Exonuclease I of *Saccharomyces cerevisiae* functions in mitotic recombination in vivo and in vitro. Mol. Cell. Biol. **17:**2764–2773.
17. **Fishman-Lobell, J., and J. E. Haber.** 1992. Removal of nonhomologous DNA ends in double-strand break recombination: the role of the yeast ultraviolet repair gene *RAD1*. Science **258:**480–484.
18. **Frank, G., J. Qiu, M. Somsouk, Y. Weng, L. Somsouk, J. P. Nolan, and B. Shen.** 1998. Partial functional deficiency of E160D flap endonuclease-1 mutant in vitro and in vivo is due to defective cleavage of DNA substrates. J. Biol. Chem. **273:**33064–33072.
19. **Freudenreich, C. H., S. M. Kantrow, and V. A. Zakian.** 1998. Expansion and length-dependent fragility of CTG repeats in yeast. Science **279:**853–856.
20. **Habraken, Y., P. Sung, L. Prakash, and S. Prakash.** 1993. Yeast excision repair gene *RAD2* encodes a single-stranded DNA endonuclease. Nature **366:**365–368.
21. **Harrington, J. J., and M. R. Lieber.** 1994. The characterization of a mammalian DNA structure-specific endonuclease. EMBO J. **13:**1235–1246.
22. **Holmes, A., and J. E. Haber.** 1999. Double-strand break repair requires both leading and lagging strand DNA polymerases. Cell **96:**415–424.
23. **Hosfield, D. J., C. D. Mol, B. Shen, and J. A. Tainer.** 1998. Structure of the DNA repair and replication endonuclease and exonuclease FEN-1: coupling DNA and PCNA binding to FEN-1 activity. Cell **95:**135–146.
24. **Hwang, Y. H., K. Baek, H.-Y. Kim, and Y. Cho.** 1998. The crystal structure of flap endonuclease-1 from *Methanococcus jannaschii*. Nat. Struct. Biol. **5:**707–713.
25. **Jinks-Robertson, S., M. Michelitch, and S. Ramcharan.** 1993. Substrate length requirements for efficient mitotic recombination in *Saccharomyces cerevisiae*. Mol. Cell. Biol. **13:**3937–3950.
26. **Johnson, R. E., G. K. Kovvali, L. Prakash, and S. Prakash.** 1998. Requirement of the yeast Rth1 5′ to 3′ exonuclease for the stability of simple repetitive DNA. Science **269:**238–239.
27. **Kokoska, R. J., L. Stefanovic, H. T. Tran, M. A. Resnick, D. A. Gordenin, and T. Petes.** 1998. Destabilization of yeast micro- and minisatellite DNA sequences by mutations affecting a nuclease involved in Okazaki fragment processing (*rad27*) and DNA polymerase δ (*pol3-t*). Mol. Cell. Biol. **18:**2779–2788.
28. **Lee, B.-S., C. P. Lichtenstein, B. Faiola, L. A. Rinckel, W. Wysock, M. J. Curcio, and D. J. Garfinkel.** 1998. Posttranslational inhibition of Ty1 retrotransposition by nucleotide excision repair/transcription factor TFIIH subunits Ssl2p and Rad3p. Genetics **148:**1743–1761.
29. **Lee, B.-S., L. Bi, D. J. Garfinkel, and A. M. Bailis.** 2000. Nucleotide excision repair/TFIIH helicases Rad3 and Ssl2 inhibit short-sequence recombination and Ty1 retrotransposition by similar mechanisms. Mol. Cell. Biol. **20:**2436–2445.
30. **Leung, K. Y., A. Malkova, and J. E. Haber.** 1997. Gene targeting by linear duplex DNA frequently occurs by assimilation of a single strand that is subject to preferential mismatch correction. Proc. Natl. Acad. Sci. USA **94:**6851–6856.
31. **Lieber, M.** 1997. The FEN-1 family of structure-specific nucleases in eukaryotic DNA replication, recombination and repair. Bioessays **19:**233–240.
32. **Lobachev, K. S., J. E. Stenger, O. G. Kozyreva, J. Jurka, D. A. Gordenin, and M. A. Resnick.** 2000. Inverted *Alu* repeats unstable in yeast are excluded from the human genome. EMBO J. **19:**3822–3830.
33. **Lovett, S. T., and V. A. Sutera, Jr.** 1995. Suppression of RecJ exonuclease mutant of *Escherichia coli* by alterations in DNA helicases II (*uvrD*) and IV (*helD*). Genetics **140:**27–45.
34. **Maines, S., M. C. Negritto, X. Wu, G. M. Manthey, and A. M. Bailis.** 1998. Novel mutations in the *RAD3* and *SSL1* genes perturb genome stability by stimulating recombination between short repeats in *Saccharomyces cerevisiae*. Genetics **150:**963–976.
35. **Manivasakam, P., S. C. Weber, J. McElver, and R. H. Schiestl.** 1995. Microhomology mediated PCR targeting in *Saccharomyces cerevisiae*. Nucleic Acids Res. **23:**2799–2800.
36. **Morrow, D. M., C. Connelly, and P. Hieter.** 1997. "Break copy" duplication a model for chromosome fragment formation in *Saccharomyces cerevisiae*. Genetics **147:**371–382.
37. **Murante, R. S., L. Rust, and R. A. Bambara.** 1995. Calf 5′ to 3′ exo/endonuclease must slide from a 5′ end of the substrate to perform structure-specific cleavage. J. Biol. Chem. **270:**30377–30383.
38. **Negritto, M. T., X. Wu, T. Kuo, S. Chu, and A. M. Bailis.** 1997. Influence of DNA sequence identity on efficiency of targeted gene replacement. Mol. Cell. Biol. **17:**278–286.
39. **Paques, F., and J. E. Haber.** 1999. Multiple pathways of recombination induced by double-strand breaks in *Saccharomyces cerevisiae*. Microbiol. Mol. Biol. Rev. **63:**349–404.
40. **Parenteau, J., and R. J. Wellinger.** 1999. Accumulation of single-stranded DNA and destabilization of telomeric repeats in yeast mutant strains carrying a deletion of *RAD27*. Mol. Cell. Biol. **19:**4143–4152.
41. **Qiu, J., M. X. Guan, A. M. Bailis, and B. Shen.** 1998. *Saccharomyces cerevisiae* exonuclease-1 plays a role in UV resistance that is distinct from nucleotide excision repair. Nucleic Acids Res. **26:**3077–3083.
42. **Reagan, M. S., C. Pittenger, W. Siede, and E. C. Friedberg.** 1995. Characterization of a mutant strain of *Saccharomyces cerevisiae* with a deletion of the *RAD27* gene, a structural homolog of the *RAD2* nucleotide excision repair gene. J. Bacteriol. **177:**364–371.
43. **Rothstein, R.** 1984. Double-strand break repair, gene conversion, and post-division segregation. Cold Spring Harbor Symp. Quant. Biol. **49:**629–638.
44. **Rothstein, R.** 1991. Targeting, disruption, replacement, and allele rescue: integrative DNA transformation in yeast. Methods Enzymol. **194:**281–301.
45. **Rothstein, R., C. Helms, and N. Rosenberg.** 1987. Concerted deletions and inversions are caused by mitotic recombination between delta sequences in *Saccharomyces cerevisiae*. Mol. Cell. Biol. **7:**1198–1207.
46. **Rubnitz, J., and S. Subramani.** 1984. The minimum amount of homology required for homologous recombination in mammalian cells. Mol. Cell. Biol. **4:**2253–2258.
47. **Sambrook, J., E. F. Fritsch, and T. Maniatis.** 1989. Molecular cloning: a laboratory manual, 2nd ed. Cold Spring Harbor Laboratory Press, Cold Spring Harbor, N.Y.
48. **Schweitzer, J. K., and D. M. Livingston.** 1998. Expansions of CAG repeat tracts are frequent in a yeast mutant defective in Okazaki fragment maturation. Hum. Mol. Genet. **7:**69–74.
49. **Shen, B., J. P. Nolan, L. A. Sklar, and M. S. Park.** 1996. Essential amino

acids for substrate binding and catalysis of human flap endonuclease 1. J. Biol. Chem. **271:**9173–9176.
50. **Shen, B., J. P. Nolan, L. A. Sklar, and M. S. Park.** 1997. Functional analysis of point mutations in human flap endonuclease-1 active site. Nucleic Acids Res. **25:**3332–3338.
51. **Shen, B., J. Qiu, D. Hosfield, and J. A. Tainer.** 1998. Flap endonuclease homologs in archaebacteria exist as independent proteins. Trends Biochem. Sci. **23:**171–173.
52. **Sherman, F., G. R. Fink, and J. B. Hicks.** 1987. Methods in yeast genetics. Cold Spring Harbor Laboratory Press, Cold Spring Harbor, N.Y.
53. **Sikorski, R. S., and P. Hieter.** 1989. A system of shuttle vectors and yeast host strains designed for efficient manipulation of DNA in *Saccharomyces cerevisiae*. Genetics **122:**19–27.
54. **Sokolsky, T., and E. Alani.** 2000. *EXO1* and *MSH6* are high-copy suppressors of conditional mutations in the *MSH2* mismatch repair gene of *Saccharomyces cerevisiae*. Genetics **155:**589–599.
55. **Sommers, C. H., E. J. Miller, B. Dujon, S. Prakash, and L. Prakash.** 1995. Conditional lethality of null mutations in *RTH1* that encodes the yeast counterpart of a mammalian 5′ to 3′ exonuclease required for lagging strand synthesis in reconstituted systems. J. Biol. Chem. **270:**4193–4196.
56. **Spiro, C., R. Pelletier, M. L. Rolfsmeier, M. J. Dixon, R. S. Lahue, G. Gupta, M. S. Park, X. Chen, S. V. S. Mariappan, and C. T. McMurray.** 1999. Inhibition of FEN-1 processing by DNA secondary structure at trinucleotide repeats. Mol. Cell **4:**1079–1085.
57. **Sugawara, N., and J. E. Haber.** 1992. Characterization of double-strand-break-induced recombination: homology requirements and single-stranded DNA formation. Mol. Cell. Biol. **12:**563–575.
58. **Sung, P., P. Reynolds, L. Prakash, and S. Prakash.** 1993. Purification and characterization of the *Saccharomyces cerevisiae* Rad1/Rad10 endonuclease. J. Biol. Chem. **26:**23691–23699.
59. **Symington, L. S.** 1998. Homologous recombination is required for the viability of *rad27* mutants. Nucleic Acids Res. **26:**5589–5595.
60. **Symington, L. S., L. E. Kang, and S. Moreau.** 2000. Alteration of gene conversion tract length and associated crossing over during plasmid gap repair in nuclease-deficient strains of *Saccharomyces cerevisiae*. Nucleic Acids Res. **28:**4649–4656.
61. **Szankasi, P., C. Gysler, U. Zehntner, U. Leupold, J. Kohli, and P. Munz.** 1986. Mitotic recombination between dispersed but related tRNA genes of *S. pombe* generates a reciprocal translocation. Mol. Gen. Genet. **202:**394–402.
62. **Thomas, B. J., and R. Rothstein.** 1989. The genetic control of direct-repeat recombination in *Saccharomyces*: the effect of *rad52* and *rad1* on mitotic recombination of a *GAL10* transcriptionally regulated gene. Genetics **123:**725–738.
63. **Tishkoff, D. X., A. L. Boerger, P. Bertrand, N. Filosi, G. M. Gaida, M. F. Kane, and R. D. Kolodner.** 1997. Identification and characterization of *Saccharomyces cerevisiae EXO1*, a gene encoding an exonuclease that interacts with *MSH2*. Proc. Natl. Acad. Sci. USA **94:**7487–7492.
64. **Tishkoff, D. X., N. Filosi, G. M. Gaida, and R. D. Kolodner.** 1997. A novel mutation avoidance mechanism dependent on *S. cerevisiae RAD27* is distinct from DNA mismatch repair. Cell **88:**253–263.
65. **Tomkinson, A. E., A. J. Bardwell, L. Bardwell, N. J. Tappe, and E. C. Friedberg.** 1993. Yeast DNA repair and recombination proteins Rad1 and Rad10 constitute a single-stranded-DNA endonuclease. Nature **362:**860–862.
66. **Tran, H. T., D. A. Gordenin, and M. A. Resnick.** 1999. The 3′→5′ exonucleases of DNA polymerases δ and ε and the 5′→3′ exonuclease Exo1 have major roles in postreplication mutation avoidance in *Saccharomyces cerevisiae*. Mol. Cell. Biol. **19:**2000–2007.
67. **Vallen, E. A., and F. R. Cross.** 1995. Mutations in *RAD27* define a potential link between G1 cyclins and DNA replication. Mol. Cell. Biol. **15:**4291–4302.
68. **Wach, A., A. Brachat, R. Pohlmann, and P. Philippsen.** 1994. New heterologous modules for classical or PCR-based disruptions in *Saccharomyces cerevisiae*. Yeast **10:**1793–1808.
69. **Wang, Z., J. Q. Svejstrup, W. J. Feaver, X. Wu, R. D. Kornberg, and E. C. Friedberg.** 1994. Transcription factor b (TFIIH) is required during nucleotide excision repair in yeast. Nature **368:**74–76.
70. **Wu, X., T. E. Wilson, and M. R. Lieber.** 1999. A role for FEN-1 in nonhomologous DNA end joining: the order of strand annealing and nucleolytic processing events. Proc. Natl. Acad. Sci. USA **96:**1303–1308.
71. **Zhu, F. X., E. E. Biswas, and S. B. Biswas.** 1997. Purification and characterization of the DNA polymerase α associated exonuclease: the *RTH1* gene product. Biochemistry **36:**5947–5954.